

Dynamics of *n*-Alkylammonium Ions Intercalated in Saponite

Miho Yamauchi,* Shin'ichi Ishimaru, and Ryuichi Ikeda

Department of Chemistry, University of Tsukuba, Tennodai 1-1-1, Tsukuba 305-8571

Received July 18, 2003; E-mail: yamauchi@staff.chem.tsukuba.ac.jp

Organo-clay composites of saponite intercalated with several kinds of *n*-alkylmono- and diammonium ions were prepared, and the dynamic properties of the intercalated cations were investigated by solid state NMR. It was found that the cationic motions are characterized by distributed correlation times due to an environmental inhomogeneity of the interlayer space of saponite.

Layered clay minerals form organo-clay composites with many kinds of organic cations. The physical and chemical properties of the composites, e.g., viscosity, dispersion, elasticity, adsorption, and catalytic ability, have been shown to depend on the kind of organic species.[1] These properties of organo-clay composites are possibly related to the low-dimensional structure and flexibility of organic species in clays.

The structures of the composites have been investigated by X-ray diffraction (XRD) studies for *n*-alkylammonium-intercalated clays,[2] and the following trends were found: the alkyl chains are placed with their long axis parallel to the inorganic sheets of clays having a small cation-exchange capacity (CEC),[1] while they are aligned with the molecular long axis tilted with certain angles to layers of clays with large CEC.[3] The molecular motions of intercalated organic cations are closely connected with the physical properties in these composites, such as the dielectric and conductive characteristics. Slight attention was, however, given to the dynamic properties of intercalated organic cations.

In previous work[4,5] we studied the molecular arrangements and motional states of *n*-octylammonium ions in the interlayer space of two kinds of layered clays, tetrasilicicfluormica and saponite. It was found that the motional properties of *n*-octylammonium ions depend on the features of the host clays, although the cationic arrangements are almost the same in both intercalation compounds. In these studies, we found that NMR is quite suitable to obtain information on the dynamic properties of microscopic states.

In this study, we intended to clarify the dynamic states of organic cations intercalated in saponite. For this purpose, *n*-alkylmono- and diammonium ions (number of carbon atom = 3, 4, 8) were chosen as intercalated cations of different types in lengths and charges; also, the motional states of these cations were investigated by solid state NMR.

Experimental

Octamethylenediammonium dichloride, *n*-butylammonium chloride, and tetramethylenediammonium dichloride were prepared by neutralizing ethanol solutions of the corresponding amines with hydrochloric acid diluted with ethanol by 1:1. The obtained crude salts were recrystallized from a mixed solvent of ethanol and diethyl ether.

Synthetic sodium-saponite (abbreviated to Na-SP), which is a reference clay of the Clay Society of Japan, and provided by Kunimine Ind. Co., was used to prepare intercalation compounds. The clay is expressed by the formula $Na_xSi_{4-x}Al_xMg_3O_{10}(OH)_2$ ($x = 0.4$) with a CEC of 70–80 meq/100 g.

Alkylammonium cations were intercalated into saponite by a conventional ion-exchange method, as follows: a fine powder of Na-SP was immersed into each aqueous solution of above-mentioned alkylammonium chlorides with the concentration adjusted to twice the CEC of Na-SP. After the exchange, products were filtered or centrifuged and washed with distilled water repeatedly until the $AgNO_3$ test became negative. Intercalated saponites with octamethylenediammonium, *n*-butylammonium and tetramethylenediammonium ions are hereafter called C82-SP, C41-SP and C42-SP, respectively. The neutralization of trimethylenediamine and the intercalation of the corresponding diammonium ions into saponite were simultaneously carried out by adding hydrochloric acid into an aqueous suspension of the amine and saponite. The obtained specimen is abbreviated as C32-SP. The deuteration of ammonium groups of the intercalated cations was carried out by keeping dried specimens under a saturated vapor of 99.5 atom% heavy water (Aldrich) at room temperature for two days. Deuterated compounds of C82-SP, C41-SP, C42-SP and C32-SP are named C82d_6-SP, C41d_3-SP, C42d_6-SP and C32d_6-SP, respectively. Since the ^{2}H spectra observed for all deuterated specimens were sufficiently strong and sharp, we can assume that a sufficient deuteration was obtained, although an accurate percentage of deuteration was not determined.

Measurements of XRD were performed for Na-SP and all intercalated compounds with a PHILIPS X'pert PW 3040 diffractometer using Cu-Kα radiation. Diffraction patterns were collected at 300 ± 2 and 400 ± 2 K.

^{2}H NMR spectra were taken for all deuterated samples at a Larmor frequency of 46.1 MHz with a Bruker MSL-300 NMR system using the quadrupole-echo sequence[6] in the temperature range 140–500 K.

The temperature dependence of ^{1}H NMR spin-lattice relaxation time was measured with a homemade apparatus using the 180°–τ–90° pulse sequence in the temperature range 100–500 K. Larmor frequencies of 15.0–54.3 MHz were employed.

Results and Discussion

Powder X-ray Diffraction. The respective intercalated specimens gave diffraction patterns for a single phase and the

Published on the web December 15, 2003; DOI 10.1246/bcsj.76.2301

Table 1. Interlayer Distances, Exchange Ratios of Alkylammonium Ions to Sodium Cations in Na-SP, and Area Fractions of the Clay Surface Covered with Intercalated Cations in Saponite Compounds

Sample	Interlayer distance[a)]/nm (Basal spacing/nm)		Exchange ratio /%	Area fraction /%
Na-saponite (Na-SP)	0.06	(1.02 ± 0.1)	—	—
$NH_3(CH_2)_8NH_3$-saponite (C82-SP)	0.41	(1.37 ± 0.1)	76	56
$CH_3(CH_2)_3NH_3$-saponite (C41-SP)	0.37	(1.33 ± 0.1)	57	50
$NH_3(CH_2)_4NH_3$-saponite (C42-SP)	0.37	(1.33 ± 0.1)	65	32
$NH_3(CH_2)_3NH_3$-saponite (C32-SP)	0.37	(1.32 ± 0.2)	67	29
$CH_3(CH_2)_7NH_3$-saponite (C81-SP)	0.39	(1.35 ± 0.1)	57	77

a) The distances were estimated from basal spacings, shown in parentheses, which are obtained from powder X-ray diffraction data at 400 K.

same diffraction pattern at 300 and 400 K. The interlayer distances for Na-SP and intercalated saponites were estimated by subtracting the layer thickness, 0.96 nm,[7] from the basal spacing derived from the (001) reflection observed at 400 K, and are listed in Table 1. The fact that interlayer distances of 0.37–0.41 nm obtained for the intercalation compounds were larger than 0.06 nm for Na-SP implies that organic cations are intercalated between clay sheets. Since the obtained interlayer distances became close to ca. 0.42 nm, estimated for the short diameter of the cross section of the alkyl chains, intercalated alkylammonium ions are expected to be arranged with their long axis parallel to the clay sheets.

The diffraction peaks of saponite were much broader than those in other kinds of synthetic clays, e.g., tetrasilicicfluormica,[5] implying that the interlayer distances in saponite compounds are widely distributed.

Elemental Analysis. From the results of elemental analyses for C, H, and N, the exchange ratio of alkylammonium ions to sodium cations in Na-SP, and the area fraction of the clay surface covered with alkylammonium ions, was estimated under consideration of van der Waals radii of the respective atoms. The obtained data are given in Table 1 together with that for octylammonium-saponite (C81-SP).[4] The area fractions determined for the samples employed in this study, which are smaller than that in C81-SP, indicate that octylammonium ions are densely packed in the interlayer space, as shown in Fig. 1(a). The percentages of C82-SP and C41-SP became ca. 70% of the value in C81-SP, as schematically shown in Fig. 1(b). The values for C42-SP and C32-SP were less than half the value of C81-SP, as depicted in Fig. 1(c). These results are consistent with a consideration of lengths and charges in intercalated cations.

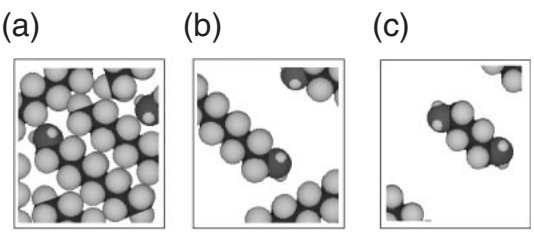

Fig. 1. Schematic arrangements of *n*-alkylammonium ions in the interlayer space of saponite: (a) $CH_3(CH_2)_7NH_3$-saponite (C81-SP), (b) $NH_3(CH_2)_8NH_3$-saponite (C82-SP), and (c) $NH_3(CH_2)_4NH_3$-saponite (C42-SP).

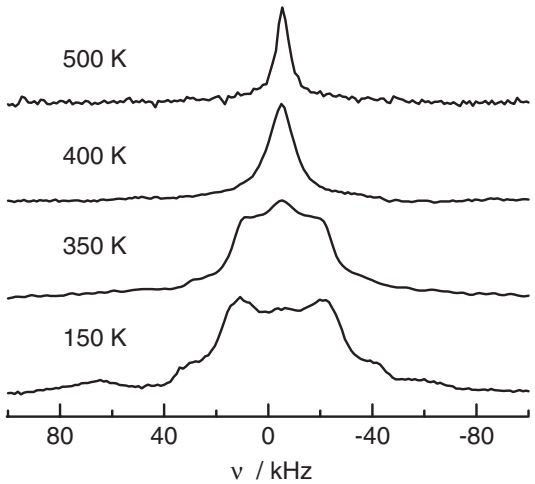

Fig. 2. A temperature dependence of ^{2}H NMR spectra observed in $ND_3(CH_2)_8ND_3$-saponite (C82d_6-SP).

^{2}H NMR Spectra. The ^{2}H NMR spectra in all of the saponite compounds studied exhibited similar temperature dependences with each other. As an example, ^{2}H spectra observed in C82d_6-SP are shown in Fig. 2. With increasing temperature, the spectral line-width was gradually narrowed. This result shows that some kind of molecular motions are excited with the temperature. It is noted that all C82d_6-SP spectra observed are broad and have tails at both sides. These results suggest that the observed spectrum is a superposition of the absorption lines with a different line-width, which implies some distribution in the crystal fields at respective cations by considering the distributed interlayer distances observed in XRD measurements.

^{2}H nuclear quadrupole coupling constants (*QCC*) were estimated from the observed ^{2}H spectra, and are shown in Fig. 3. Since it is difficult to obtain the exact *QCC* values for the spectra with a Gaussian-like shape, a *QCC* was roughly estimated from the line-width in the high-temperature region. *QCC* values of 50–56 kHz were obtained at ca. 150 K. These values are approximately the same as 58 kHz calculated for the rotating ND_3^+ group about its C_3 axis by assuming that the reduction factor $(1 - 3\cos^2\Theta)/2$, where Θ is the angle between the principal axis of the electric field gradient at deuterons and the rotational axis for a molecular motion and by using the *QCC* of 173 kHz reported for the rigid ND_3^+ group in ethylammonium chloride.[8] This ND_3^+ motional mode is abbreviated as [ND_3^+-rot]. The existence of a narrow component implies

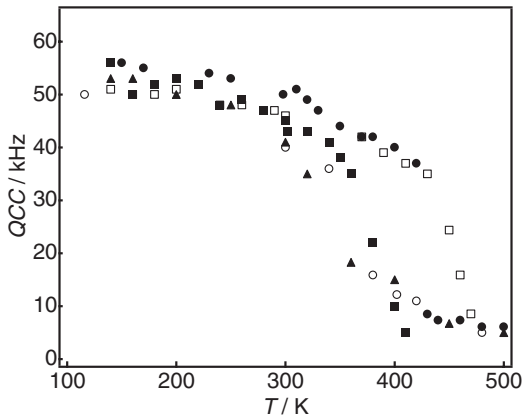

Fig. 3. Temperature dependences of ^{2}H nuclear quadrupole coupling constants determined from the line-width of ^{2}H NMR spectra observed in $ND_3(CH_2)_8ND_3$-saponite (C82d_6-SP, ●), $CH_3(CH_2)_3ND_3$-saponite (C41d_3-SP, □), $ND_3(CH_2)_4ND_3$-saponite (C42d_6-SP, ■), and $ND_3(CH_2)_3ND_3$-saponite (C32d_6-SP, ▲).

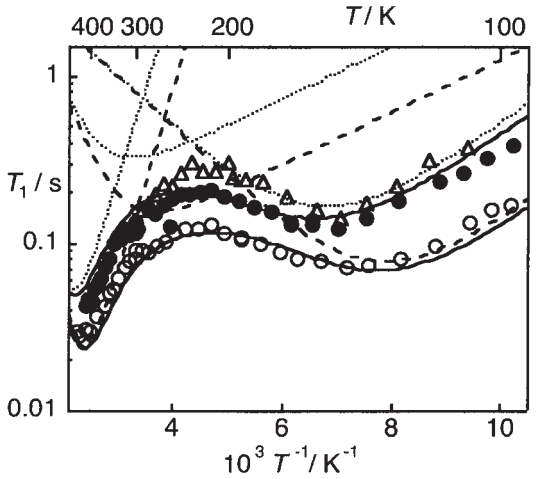

Fig. 4. ^{1}H NMR spin-lattice relaxation times T_1 observed for $CH_3(CH_2)_3NH_3$-saponite (C41-SP) at 54.3 MHz (●) and 25.6 MHz (○), and for $CH_3(CH_2)_3ND_3$-saponite (C41d_3-SP) at 54.3 MHz (△). Dotted and broken lines are respective T_1 components calculated at 54.3 and 25.6 MHz and these superpositions are expressed by solid lines.

the excitation of a motional mode other than [ND_3^+-rot]. In the temperature range 200–350 K, *QCC* of the broad component gradually decreased to ca. 35 kHz. Considering the XRD results, that the interlayer distances are almost the same between 300 and 400 K, the cationic uniaxial rotation as a whole [Uniaxis-rot], which causes no expansion of the interlayer distances, is expected to be excited in this temperature region. It is noted that the observed quite gradual *QCC* reduction is unusual as a thermal excitation of molecular motions, and that the observed *QCC* value was larger than the calculated value of 22 kHz for [Uniaxis-rot]. Since the distributions of the interlayer distances were observed, it is highly provable that the motional correlation time of [Uniaxis-rot] is distributed in the saponite specimens.

In the temperature range 350–500 K, the *QCC* decreased from ca. 35 kHz to ca. 5 kHz in all compounds. Since there is no change in the interlayer distance between 300 and 400 K, this *QCC* reduction is highly assignable to cationic rotation around an axis perpendicular to the long axis [Plane-rot]. The *QCC* values for [Plane-rot] are estimated to be ca. 11 kHz. Since the observed *QCC* was somewhat smaller than the calculated one, the [Plane-rot] seems to take place together with a small fluctuation of the rotational axis for this mode. It is noteworthy that this [Plane-rot] is a unique motional mode only detectable in the 2-D system, and has not been reported in bulk crystals.

^{1}H NMR Spin-Lattice Relaxation Time (T_1). ^{1}H NMR spin-lattice relaxation times (T_1) for C41-SP measured at 54.3 and 25.6 MHz, and C41d_3-SP at 54.3 MHz are shown in Fig. 4. Below 300 K, the T_1 values for C41-SP and C41d_3-SP were nearly the same, except for those in the range 160–300 K, where T_1 in C41d_3-SP was longer than that in C41-SP. The T_1 relaxation in C41-SP in this temperature range is attributable to the motions of the ND_3^+ groups, because longer T_1 values in C41d_3-SP are explainable by less-averaged dipolar interactions by this motion. A deep minimum observed in both analogs below 160 K can be assigned to the CH_3-rotation around the C_3-axis [CH_3-rot]. Above 300 K, the T_1 for C41-SP decreased monotonously with a frequency dependency. The T_1 measured at 25.6 MHz gave a minimum at ca. 400 K. By considering the *QCC* results, the T_1 decrease is attributable to [Uniaxis-rot]. In the case that ^{1}H relaxation is caused by molecular motions, T_1 is expressed by the BPP-type equation,[9] given by

$$\frac{1}{T_1^{\mathrm{BPP}}} = \frac{2}{3}\gamma^2 \Delta M_2 \left\{ \frac{\tau}{1+\omega_0^2\tau^2} + \frac{4\tau}{1+4\omega_0^2\tau^2} \right\}, \qquad (1)$$

where γ, ΔM_2, ω_0, and τ are the gyromagnetic ratio of a proton, the reduction in the second moment M_2 of the NMR absorption by the onset of the motion, the angular Larmor frequency, and the motional correlation time, respectively. The motional correlation time (τ) usually follows the Arrenius-type formula, given by

$$\tau = \tau_\infty \exp\left(\frac{E_a}{RT}\right), \qquad (2)$$

where τ_∞ and E_a are the motional correlation time in the limit of the infinite temperature and the activation energy for the motion, respectively. The temperature dependences of T_1 for C41-SP were fitted by using Eqs. 1 and 2. The reproduction of the observed T_1 curves, however, was poor in the frequency dependence over the whole temperature region studied. Especially, the ΔM_2 of 1.5×10^{-2} mT^2, estimated for the C_3-rotation of NH_3^+ groups, [NH_3^+-rot], did not agree with the calculated 3.7×10^{-2} mT^2. Some synthesized clays are made from natural clay, while the saponite in the present study was synthesized hydrothermally only with artificial sources. This implies that no paramagnetic impurities existed in the present saponite. We, therefore, ignore the influence of paramagnetic impurities on the T_1 behavior in our saponite specimens. Taking into account the discussion on ^{2}H *QCC*, we introduce a Cole–Davidson type distribution, $g(\tau)$, in the motional correlation time (τ), given by

$$g(\tau) = \frac{\sin\beta\pi}{\pi}\left(\frac{\tau}{\tau_0 - \tau}\right)^{\beta} \quad \text{for } \tau \leq \tau_0$$
$$\text{and} = 0 \quad \text{for } \tau > \tau_0. \tag{3}$$

The value of β ($0 < \beta \leqq 1$) is a measure of the distribution, where $\beta = 1$ expresses no distribution in τ, and τ_0 is the long limit of τ.[10] Applying this distribution, T_1 can be rewritten as

$$\frac{1}{T_1^{\text{dis}}} = \frac{2}{3}\gamma^2\Delta M_2\left\{\frac{\tau_0 \sin(\beta\tan^{-1}\omega\tau_0)}{\omega\tau_0(1+\omega^2\tau_0^2)^{\beta/2}} + \frac{2\tau_0 \sin(\beta\tan^{-1}2\omega\tau_0)}{\omega\tau_0(1+4\omega^2\tau_0^2)^{\beta/2}}\right\}. \tag{4}$$

The observed T_1 curves were reproduced by summing the theoretical curves calculated for each motional mode by using Eqs. 3 and 4, as shown in Fig. 4. The estimated motional parameters are given in Table 2. The ΔM_2 value of 4.0×10^{-2} mT^2, evaluated for the T_1 in the range 160–300 K, is reasonable for the excitation of [NH^{3+}-rot]. This result implies that crystal fields at the $NH_3{}^+$ groups are not homogeneous, but are distributed in accordance with the foregoing gradual *QCC* reductions.

The T_1 observed in C82-SP and C42-SP exhibited a similar temperature dependence with each other. As a representative, T_1 curves in C82-SP and C82d_6-SP are shown in Fig. 5. Below 300 K, the T_1 could be fitted by the superposition of two T_1 minima calculated by using Eqs. 3 and 4. Since the T_1 values in C82d_6-SP were longer than those in C82-SP in this temperature range, the two T_1 minima were attributed to the $NH_3{}^+$ motions. Above 300 K, a T_1 decrease was observed in C82-SP and is ascribable to [Uniaxis-rot] by referring to the analysis of C41-SP. The E_a for this mode in C82-SP was estimated from the slopes of $\ln T_1$ vs T^{-1}. The T_1 data in C42-SP could be reproduced in the same manner as those in C82-SP. All motional parameters derived from the T_1 analysis for C82-SP and C42-SP are given in Table 2.

The T_1 curve observed for C32-SP below 300 K could be reproduced with a single minimum calculated by using Eqs. 3 and 4, which is attributable to [$NH_3{}^+$-rot], while the T_1 curves for C42-SP and C82-SP were explained by the superposition of two T_1 minima.

Table 2. Fitting Parameters of ^{1}H NMR Spin-Lattice Relaxation Times Observed in Samples of *n*-Alkylammonium-Saponite: Motional Modes, Activation Energies (E_a), and Parameters Presenting the Width of τ Distribution (β)

Compound	Motional mode	E_a/kJ mol^{-1}	β
$NH_3(CH_2)_8NH_3$-saponite (C82-SP)	$NH_3{}^+$-rot	9.4 ± 2	0.2
		14 ± 3	0.2
	Uniaxis-rot	32 ± 8	—
$CH_3(CH_2)_3NH_3$-saponite (C41-SP)	CH_3-rot	5.7 ± 0.7	0.8
	$NH_3{}^+$-rot	15 ± 3	0.2
	Uniaxis-rot	33 ± 3	0.7
$NH_3(CH_2)_4NH_3$-saponite (C42-SP)	$NH_3{}^+$-rot	7.4 ± 3	0.2
		14 ± 3	0.2
	Uniaxis-rot	30 ± 5	—
$NH_3(CH_2)_3NH_3$-saponite (C32-SP)	$NH_3{}^+$-rot	9.3 ± 2	0.2
	Uniaxis-rot	24 ± 4	—

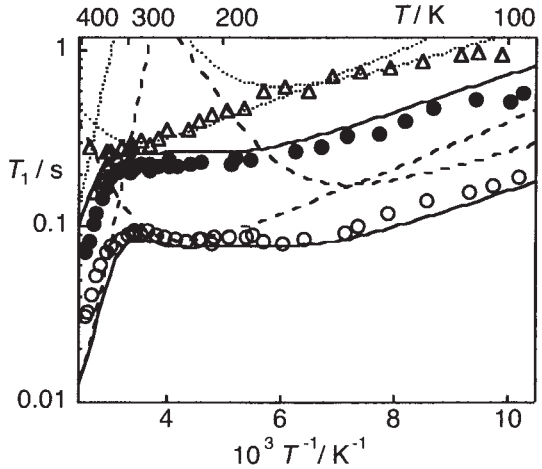

Fig. 5. ^{1}H NMR spin-lattice relaxation times T_1 observed for $NH_3(CH_2)_8NH_3$-saponite (C82-SP) at 54.3 MHz (●) and 15.0 MHz (○) and for $ND_3(CH_2)_8ND_3$-saponite (C82d_6-SP) at 54.3 MHz (△). Dotted and broken lines are respective T_1 components calculated at 54.3 and 15.0 MHz and these superpositions are expressed by solid lines.

As can be seen in Table 2, all specimens show quite small β values of 0.2 for [$NH_3{}^+$-rot], implying that the environment around organic cations in saponite is highly inhomogeneous. It is noted that two kinds of activation energies were obtained for [$NH_3{}^+$-rot] in C82-SP and C42-SP. In the case of C82-SP and C42-SP, because of the relatively long distances between the terminal ammonium groups, it is acceptable that both terminals cannot be located at the position near to an anion of the host, resulting in a large environmental inhomogeneity around the terminal groups. On the other hand, a single activation energy was obtained in C32-SP. This can be explained by the short cationic length of a trimethylenediammonium ion; namely, both terminals can stay close to an anion.

The activation energies for [Uniaxis-rot] were independent of the charges on the intercalated cations. Considering the fact that the cationic environment should be inhomogeneous in the interlayer spaces of saponite, it is likely that the environmental inhomogeneity is a more dominant factor on the excitation of the cationic uniaxial rotation than the difference in the alkylammonium ions.

Conclusion

From an XRD analysis, the averaged arrangements of intercalated alkylammonium ions with alkyl chains of C_2–C_8 and mono- and diammonium groups in saponite having a 2-D layer structure was found to be almost the same in all specimens, i.e., the molecular long axes are parallel to the 2-D plane of the clay. In NMR studies, the motional states of intercalated alkylammonium ions were characterized with distributed motional correlation times. This distribution is expected to come from the inhomogeneity of the crystal field caused by the distribution of the interlayer distance and the distance between the cations and the anion centers of layers of saponite. In all of the compounds employed in this study, the cationic mode of [Plane-rot] was observed. It is notable that because this mode has not been

observed in other three-dimensional crystalline salts, it is a characteristic of the 2-D space of layered clay minerals.

References

1 G. Lagaly, *Clay Miner.*, **16**, 1 (1981).

2 A. Weiss, *Angew. Chem.*, **75**, 113 (1963).

3 G. F. Walker, *Clay Miner.*, **7**, 129 (1967).

4 M. Yamauchi, S. Ishimaru, and R. Ikeda, *Mol. Cryst. Liq. Cryst. Sci. Technol., Sect. A*, **341**, 315 (2000).

5 M. Yamauchi, S. Ishimaru, and R. Ikeda, *Z. Naturforsch., A: Phys. Sci.*, **54**, 755 (1999).

6 J. H. Davis, K. P. Jeffrey, M. Bloom, M. F. Valic, and T. P. Higgs, *Chem. Phys. Lett.*, **42**, 390 (1976).

7 T. Endo, T. Sato, and M. Shimada, *J. Phys. Chem. Solids*, **47**, 799 (1986).

8 M. J. Hunt and A. L. Mackay, *J. Magn. Reson.*, **15**, 402 (1974).

9 A. Abragam, "The Principles of Nuclear Magnetism," Oxford University Press, London (1967).

10 D. W. Davidson and R. H. Cole, *J. Chem. Phys.*, **19**, 1484 (1951).